# Characterization of Kinetic Folding Intermediates of Recombinant Canine Milk Lysozyme by Stopped-Flow Circular Dichroism†

Masaharu Nakao,‡ Kosuke Maki,‡ Munehito Arai,§ Takumi Koshiba,||,⊥ Katsutoshi Nitta,|| and Kunihiro Kuwajima*,‡

*Department of Physics, School of Science, University of Tokyo, 7-3-1 Hongo, Bunkyo-ku, Tokyo 113-0033, Japan, Institute for Biological Resources and Functions, National Institute of Advanced Industrial Science and Technology, 1-1-1 Higashi, Tsukuba, Ibaraki 305-8566, Japan, and Division of Biological Sciences, Graduate School of Science, Hokkaido University, N10 W8, Kita-ku, Sapporo, Hokkaido 060-0810, Japan*

*Received January 14, 2005; Revised Manuscript Received March 2, 2005*

ABSTRACT: The intermediate in the equilibrium unfolding of canine milk lysozyme induced by a denaturant is known to be very stable with characteristics of the molten globule state. Furthermore, there are at least two kinetic intermediates during refolding of this protein: a burst-phase (first) intermediate formed within the dead time of stopped-flow measurements and a second intermediate that accumulates with a rate constant of 22 $s^{-1}$. To clarify the relationships of these intermediates with the equilibrium intermediate, and also to characterize the structural changes of the protein during refolding, here we studied the kinetic refolding reactions using stopped-flow circular dichroism at 10 different wavelengths and obtained the circular dichroism spectra of the intermediates. Comparison of the circular dichroism spectra of the intermediates, as well as the absence of observed kinetics in the refolding from the fully unfolded state to the equilibrium intermediate, has demonstrated that the burst-phase intermediate is equivalent to the equilibrium intermediate. The difference circular dichroism spectrum that represented changes from the kinetic intermediate to the native state had characteristics of an exciton coupling band, indicating that specific packing of tryptophan residues in this protein occurred in this phase. From these findings, we propose a schematic model of the refolding of canine milk lysozyme that is consistent with the hierarchical mechanism of protein folding.

Protein folding is the process by which one-dimensional genetic information encoded as an amino acid sequence is translated into a specific, native tertiary structure that has biological activity in vivo. Protein folding is a fundamental process of biological phenomena, and hence, elucidation of the mechanism of folding is an important issue of molecular biology (*1*).

Since the 1970s, the folding pathways of proteins have been studied extensively. Observation of an equilibrium unfolding intermediate and its possible relationship to the intermediate of folding have been reported for many globular proteins. The equilibrium intermediate has common characteristics among different globular proteins: (1) It has nativelike secondary structure. (2) The size of the molecule is compact with a radius 10−30% larger than that in the native state. (3) The tight packing of side chains in the molecule is lost, but the tertiary fold of the main chain is partly retained. The equilibrium intermediate may be a common physical state of globular proteins, and is often called the "molten globule" state. It has also been shown that the molten globule state accumulates at an early stage of refolding, often within the dead time of a stopped-flow apparatus (a few milliseconds), and that the protein subsequently refolds to the native state (*2*). It is suggested that the molten globule state is a general intermediate of protein folding (*3*−*5*). For this reason, precise characterization of the molten globule and its relationship with the folding intermediate is a fundamental strategy of experimental studies of protein folding.

Canine milk lysozyme is a $Ca^{2+}$-binding *c*-type lysozyme that contains 129 amino acid residues and has a molecular weight of 14 600, and a crystallographic study has shown that the structure of this protein is very similar to those of other lysozymes and α-lactalbumin (*6*); hence, it is composed of two domains, an α-domain and a *β*-domain. The α-domain mainly consists of four α-helices, and the *β*-domain is formed by a series of loops and three antiparallel *β*-strands (see Figure 6).

An equilibrium thermal unfolding study has shown that canine lysozyme exhibits a molten globule-like intermediate with a structure that is more stable and nativelike than those of other lysozymes and α-lactalbumin (*6*). The structured intermediate also accumulates in the equilibrium unfolding induced by guanidine hydrochloride (GdnHCl),[1] and the observed intermediate is thermodynamically more stable than those of equine milk lysozyme and bovine α-lactalbumin (*7*, *8*). In the kinetic refolding of canine milk lysozyme from

† This work was supported by Grants-in-Aid for Scientific Research in Priority Areas (15076201) from the Ministry of Education, Culture, Science and Technology of Japan.

* To whom correspondence should be addressed. Phone: +81-3-5841-4128. Fax: +81-3-5841-4512. E-mail: kuwajima@ phys.s.u-tokyo.ac.jp.

‡ University of Tokyo.

§ National Institute of Advanced Industrial Science and Technology.

|| Hokkaido University.

⊥ Present address: Division of Biology, California Institute of Technology, 1200 E. California Blvd., MC114-96, Pasadena, CA 91125.

10.1021/bi050082+ CCC: $30.25 
Published on Web 04/07/2005

the GdnHCl-induced unfolded state, there were at least two kinetic intermediates observed; a burst-phase (first) intermediate accumulated within 4 ms, that is, the dead time of the measurement, and a second intermediate was observed during the kinetics with a rate constant of 10−20 $s^{-1}$ after the burst phase (*8*). The second intermediate has so far been observed only in canine milk lysozyme, and the other lysozymes and α-lactalbumin are known to accumulate only the burst-phase intermediate during kinetic refolding. The molten globule state in these other proteins observed in the equilibrium GdnHCl-induced unfolding is known to be identical with the burst-phase intermediates (*2*, *9*). Thus, it is interesting to investigate which intermediate, the burst-phase or second intermediate, corresponds to the equilibrium intermediate, and what structural changes are observed in every phase in the refolding of canine lysozyme from the fully unfolded to the native state. Because the characteristics of the intermediates observed in canine milk lysozyme are distinctive among those in the lysozyme and α-lactalbumin family, the characterization of the folding reaction of canine milk lysozyme may provide a key to understanding possible general folding mechanisms of the proteins in this family.

In this study, we have investigated the kinetic refolding of recombinant canine milk lysozyme by means of circular dichroism (CD) at 10 different wavelengths with a stopped-flow technique, and obtained the CD spectra of the burst-phase and second kinetic intermediates observed during the refolding process. From a comparison of the spectrum of the pure equilibrium intermediate with those of the two kinetic intermediates, and also from the rapidity of the CD change from the unfolded state to the equilibrium intermediate, it is found that the burst-phase intermediate is equivalent to the equilibrium unfolding intermediate. The kinetic difference CD spectra between the second intermediate and the final native state indicated an exciton contribution of adjacent tryptophan residues in the peptide CD region, suggesting that the specific tight packing of the tryptophan residues may take place at the final stage of refolding of the protein.

## MATERIALS AND METHODS

*Reagents.* GdnHCl was of specially prepared reagent grade and was obtained from Nacalai Tesque, Inc. (Kyoto, Japan). All other chemicals were of guaranteed reagent grade. The concentration of GdnHCl was determined by an Atago 3T refractometer using the following equation (*10*):

$$[\mathrm{GdnHCl}] = 57.147(\Delta N) + 38.68(\Delta N)^2 - 91.60(\Delta N)^3$$

where $\Delta N$ and [GdnHCl] are the refractive index increment at 25 °C and the concentration of GdnHCl, respectively. The concentration of canine milk lysozyme was determined spectrophotometrically at 280 nm with an extinction coefficient of $E_{1\%}^{1\mathrm{cm}} = 23.2$ (*11*).

[1] Abbreviations: CD, circular dichroism; DHFR, dihydrofolate reductase; DTT, dithiothreitol; EDTA, ethylenediaminetetraacetic acid; GdnHCl, guanidine hydrochloride; HEPES, 4-(2-hydroxyethyl)-1-piperazineethanesulfonic acid; HPLC, high-performance liquid chromatography; I, equilibrium unfolding intermediate; $I_{burst}$, burst-phase intermediate; $I_{second}$, second kinetic intermediate; N, native state; NMR, nuclear magnetic resonance; TFA, trifluoroacetic acid; U, unfolded state.

*Expression and Purification of Canine Milk Lysozyme.* The expression and purification of recombinant canine milk lysozyme were performed as described previously (*8*). In addition to these previously described protocols, we used the following protocols to purify and refold the protein. The inclusion bodies expressed in *Escherichia coli* cells were suspended in 6 M GdnHCl containing 50 mM Tris-HCl (pH 8.0), 1 mM ethylenediaminetetraacetic acid (EDTA), and 0.1 M dithiothreitol (DTT), and kept at room temperature overnight. The unsolubilized debris was removed by centrifugation, and the solubilized protein was partially purified by gel filtration on a column of Sephacryl S-100 (ϕ, 50 mm × 870 mm) equilibrated with an equilibration buffer [50 mM Tris-HCl, 1 mM EDTA, 7 M urea, 3.5 M $LiCl_2$, and 1 mM DTT (pH 8.0)]. The fractions containing lysozyme were pooled and used for refolding.

The refolding of the canine lysozyme that had been partially purified by gel filtration was carried out using gel filtration chromatography. The protein was first dialyzed against 0.1 M acetic acid and precipitated. The precipitate was collected by centrifugation, and resolubilized in 6 M GdnHCl, 0.1 M acetic acid, and 1 mM DTT. The solubilized protein was refolded by applying the solution to a column of Sephacryl S-100 (ϕ, 50 mm × 870 mm) equilibrated with the refolding buffer [3 mM reduced glutathione, 0.3 mM oxidized glutathione, 50 mM Tris-HCl, and 1 mM $CaCl_2$ (pH 8.0)]. The fractions containing bacteriolytic activity were collected and dialyzed against 20 mM 4-(2-hydroxyethyl)-1-piperazineethanesulfonic acid (HEPES) buffer with 1 mM $CaCl_2$ at pH 7.0.

The refolded protein was further purified with an SP-Sepharose FF column (ϕ, 26.4 mm × 460 mm) equilibrated with 20 mM HEPES buffer (pH 7.0) that contained 1 mM $CaCl_2$. The protein was eluted from the column with a linear gradient of NaCl from 0 to 0.3 M (4 column volumes). The fractions containing the protein were collected and applied to a reverse-phase high-performance liquid chromatography (HPLC) Octadecyl 4-PW column (ϕ, 55 mm × 200 mm) (Tosoh Co., Tokyo, Japan) at room temperature with a gradient of acetonitrile from 32 to 37% in 125 min using 0.1% trifluoroacetic acid (TFA) in distilled water and 0.07% TFA in acetonitrile. The fractions that contained the purified protein were collected and lyophilized.

*Equilibrium Experiments and Calculation of the Fraction of Each State.* Equilibrium CD spectra were measured using a Jasco J-720 spectropolarimeter. Samples were prepared in 50 mM sodium cacodylate buffer (pH 7.0) that contained 50 mM NaCl, 1 mM $CaCl_2$, and the indicated concentrations of GdnHCl. The path lengths of optical cuvettes were 2.0 and 10.0 mm for the far- and near-ultraviolet (UV) CD measurements, respectively. The temperature of the cuvette was controlled at 25 °C by circulating water. The concentration of lysozyme was 5.5−5.6 μM.

The fractions of three states {the native state [$f_N(c)$], the intermediate state [$f_I(c)$], and the unfolded state [$f_U(c)$]} of canine milk lysozyme, equine milk lysozyme, and bovine α-lactalbumin were calculated by the following formula:

$$f_N(c) = \frac{1}{1 + \exp[-(\Delta G_{NI}^{H_2O} - m_{NI}c)/RT] + \exp[-(\Delta G_{NU}^{H_2O} - m_{NU}c)/RT]}$$

$$f_I(c) = \frac{\exp[-(\Delta G_{NI}^{H_2O} - m_{NI}c)/RT]}{1 + \exp[-(\Delta G_{NI}^{H_2O} - m_{NI}c)/RT] + \exp[-(\Delta G_{NU}^{H_2O} - m_{NU}c)/RT]}$$

$$f_U(c) = \frac{\exp[-(\Delta G_{NU}^{H_2O} - m_{NU}c)/RT]}{1 + \exp[-(\Delta G_{NI}^{H_2O} - m_{NI}c)/RT] + \exp[-(\Delta G_{NU}^{H_2O} - m_{NU}c)/RT]} \quad (1)$$

where $\Delta G_{NI}^{H_2O}$ and $\Delta G_{NU}^{H_2O}$ are the free energy changes between the native (N) and the intermediate (I) state and between N and the unfolded (U) state at 0 M GdnHCl, respectively, and $m_{NI}$ and $m_{NU}$ represent the cooperativity indices of the transitions. For the calculations, we used the values of the free energy changes and the cooperativity indices reported previously (*8*, *9*, *12*).

*Kinetic Experiments.* Kinetic far-UV CD measurements were carried out using a stopped-flow apparatus (specially designed and constructed by Unisoku Co., Ltd., Osaka, Japan) installed in the cell compartment of the Jasco J-720 spectropolarimeter (*2*). All kinetics were measured in the presence of 50 mM sodium cacodylate, 50 mM NaCl, and 1 mM $CaCl_2$ at pH 7.0. The temperature was controlled at 25 °C by circulating water. The reactions were initiated by mixing the protein solution with buffers at various concentrations of GdnHCl. The mixing ratio of the protein solution to the buffer was 1:10.4. The path lengths of the optical cell were 3.8 and 1.0 mm for the refolding and unfolding measurements, respectively. The dead times of the refolding and unfolding measurements were 25 and 15 ms, respectively. The final concentration of the protein was 4.3−6.3 $\mu$M.

The observed kinetic curves were fitted to the following equation by the nonlinear least-squares method:

$$A(t) = A_\infty + \sum_i A_i \exp(-k_i t) \quad (2)$$

where $A(t)$ and $A_\infty$ are the signal values at time $t$ and infinite time, respectively, and $A_i$ and $k_i$ are the amplitude and apparent rate constant of phase $i$, respectively. In the analysis of the kinetic refolding curves, we performed global fitting using Sigmaplot 8 (Systat Software Inc., Richmond, CA), in which the 10 kinetic curves at different wavelengths were fitted simultaneously. The kinetics were biphasic, so the fitting variables were $k_1$, $k_2$, and 10 sets of $A_\infty$, $A_1$, and $A_2$.

## RESULTS

*Equilibrium Measurements.* Figure 1a shows the fractions of the native (N), intermediate (I), and unfolded (U) states of canine milk lysozyme as a function of GdnHCl at 1.0 mM $CaCl_2$ at pH 7.0 and 25 °C. These fractions were calculated from the thermodynamic parameters of the unfolding transition of the protein previously estimated by CD and fluorescence measurements (*8*). The midpoints of the unfolding transitions from N to I and from I to U are observed at GdnHCl concentrations of 2.9 and 4.9 M, respectively, and the I state is most prevalent (84%) at 3.85 M GdnHCl. Equine milk lysozyme and bovine α-lactalbumin also undergo the three-state equilibrium unfolding transition in GdnHCl under similar experimental conditions (*9*, *12*).

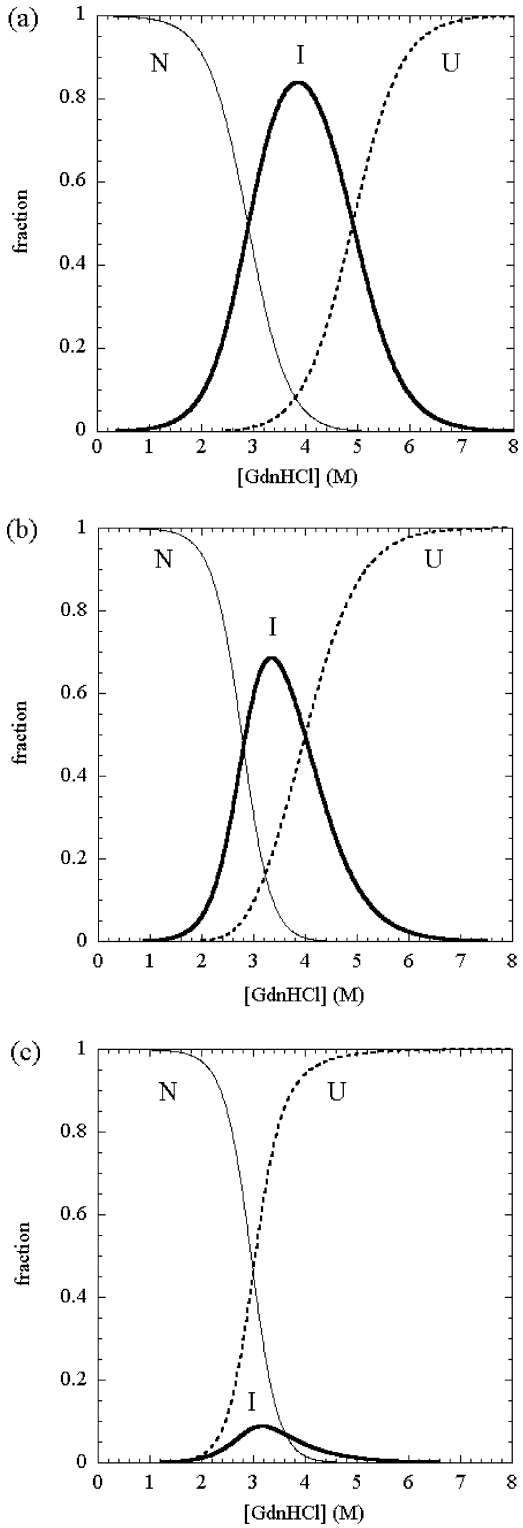


FIGURE 1: GdnHCl dependence of the fraction of the native (N, thin solid line), the intermediate (I, thick solid line), and the unfolded (U, dashed line) states of (a) canine milk lysozyme, (b) equine milk lysozyme, and (c) bovine α-lactalbumin. The fraction of each state is calculated using the equilibrium unfolding parameter values reported previously (*8*, *9*, *11*).

In both proteins, however, the GdnHCl concentration and the percent fraction of the intermediate at which the intermediate is maximally populated are both lower than those of canine lysozyme: 3.34 M GdnHCl and 69% for equine lysozyme and 3.17 M GdnHCl and 8.9% for bovine α-lactalbumin (Figure 1b,c).

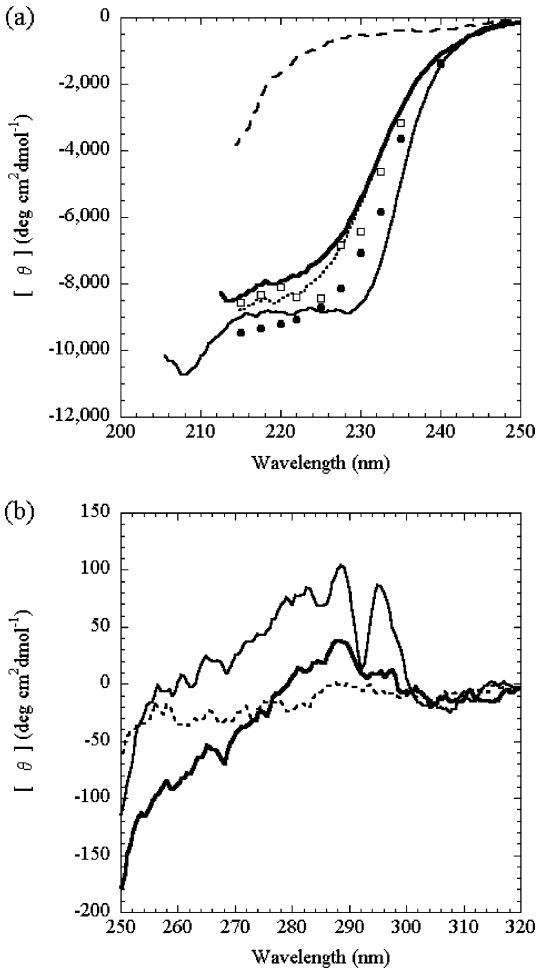


FIGURE 2: CD spectra of canine lysozyme in (a) the far-UV and (b) near-UV regions. The spectra of lysozyme in the native (0 M GdnHCl; thin solid line), intermediate (3.85 M GdnHCl; thick solid line), and unfolded (7.14 M GdnHCl; broken line) states are shown. The dotted line in panel a represents the spectrum of the pure intermediate state at 3.85 M GdnHCl calculated from the observed spectra at GdnHCl concentrations of 0, 3.85, and 7.14 M (see the text). Empty squares show the ellipticity values for the burst-phase intermediate, and filled circles show the ellipticity values of the second kinetic intermediate.

Figure 2 shows the CD spectra of canine lysozyme at 0, 3.85, and 7.14 M GdnHCl with 1.0 mM $CaCl_2$ at pH 7.0 and 25 °C. The spectra in the N state at 0 M GdnHCl and in the U state at 7.14 M GdnHCl are in good agreement with those previously reported (*8*). The far-UV CD spectrum at 3.85 M GdnHCl exhibits a large negative ellipticity from 215 to 230 nm. This result is consistent with the presence of α-helical secondary structures in the I state. The near-UV CD spectrum at 3.85 M GdnHCl shows small positive peaks at 289 and 295 nm and a shoulder at 280 nm, although these peaks and the shoulder are less pronounced than those observed in the N state. Thus, the specific tertiary packing structures of aromatic side chains may be partly retained in the I state.

*Kinetic Folding and Unfolding Reactions.* Panels a and b of Figure 3 show the refolding curves measured by stopped-flow CD experiments at 220 and 232.5 nm. The refolding reaction of lysozyme was induced by a GdnHCl concentration jump from 7 to 0.61 M by the stopped-flow mixing technique, and the resultant kinetics were observed by rapid CD measurements. The ellipticity values extrapolated to time zero are much lower (i.e., the intensities are much larger) than those of the U state (see Figure 2a), indicating that there must be a burst phase occurring within the dead time of the stopped-flow instrument (25 ms). The observed kinetics are

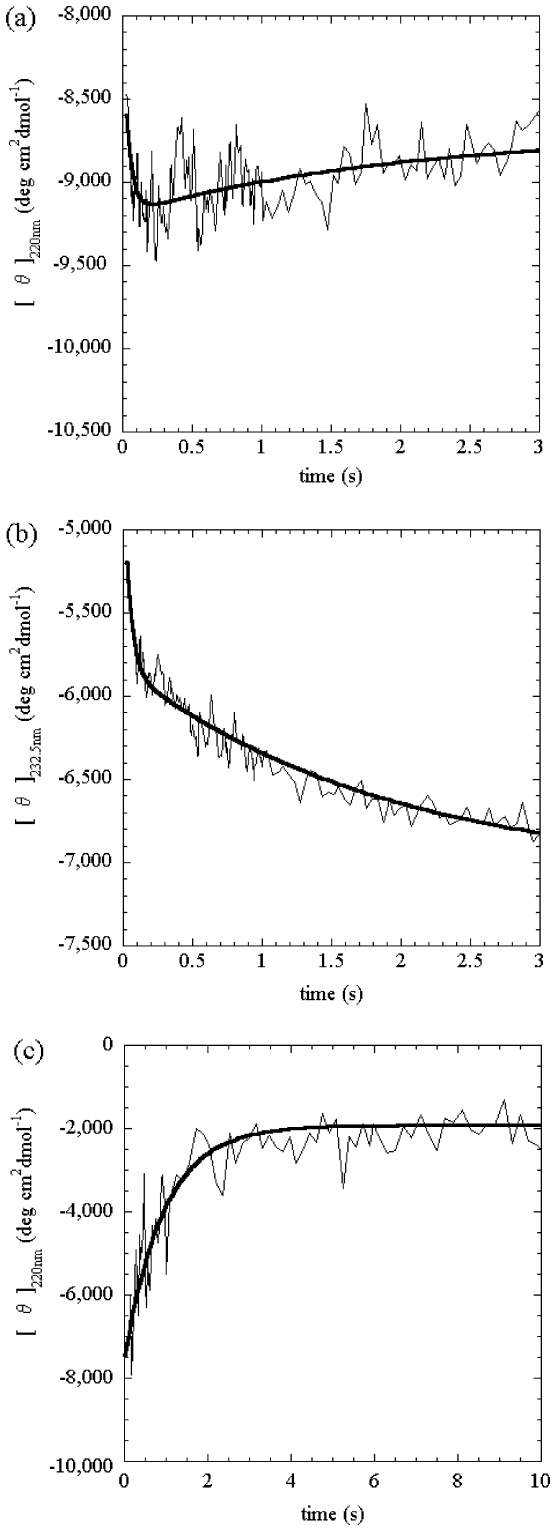


FIGURE 3: Kinetic refolding curves of canine lysozyme measured by far-UV CD at (a) 220 and (b) 232.5 nm. The reaction was initiated by a GdnHCl concentration jump from 7 to 0.61 M. Thick solid lines represent the theoretical curves fitted to two exponentials calculated by the global fitting. (c) A kinetic unfolding curve of canine lysozyme measured by far-UV CD at 220 nm. The reaction was initiated by a GdnHCl concentration jump from 0 to 7.66 M. The thick solid line represents the theoretical curve fitted to one exponential calculated by the nonlinear least-squares method.

Table 1: Amplitudes of the Two Phases in Refolding of Canine Milk Lysozyme

| wavelength (nm) | $A_\infty$[a] (deg cm$^2$ dmol$^{-1}$) | $A_1$[b] (deg cm$^2$ dmol$^{-1}$) ($k_1 = 22 \pm 2$ s$^{-1}$) | $A_2$[b] (deg cm$^2$ dmol$^{-1}$) ($k_2 = 0.53 \pm 0.02$ s$^{-1}$) |
|---|---|---|---|
| 215 | −8863.3 | 900 ± 200 | −610 ± 20 |
| 217.5 | −8724.5 | 1000 ± 200 | −590 ± 20 |
| 220 | −8710.0 | 1100 ± 200 | −480 ± 20 |
| 222 | −8551.2 | 700 ± 200 | −510 ± 20 |
| 225 | −8499.9 | 300 ± 100 | −210 ± 20 |
| 227.5 | −8349.5 | 1300 ± 200 | 210 ± 20 |
| 230 | −7894.7 | 600 ± 200 | 820 ± 20 |
| 232.5 | −7072.2 | 1200 ± 200 | 1250 ± 20 |
| 235 | −4444.8 | 500 ± 100 | 810 ± 20 |
| 240 | −1403.9 | 300 ± 100 | 20 ± 20 |

[a] The values of $A_\infty$ shown above were obtained by the nonlinear least-squares method at individual wavelengths, and then the values were fixed during the global nonlinear least-squares fitting of the parameters (the two rate constants common at every wavelength, and the two amplitudes at each wavelength). [b] The parameter values and their standard errors are shown.

biphasic, as represented by two exponential terms using nonlinear least-squares calculation, suggesting that there must be a second kinetic intermediate ($I_{second}$) in addition to the burst-phase (first) intermediate ($I_{burst}$) during refolding of the protein. In the measurement at 220 nm, the overshoot of the ellipticity was observed in the first observable phase of the biphasic kinetics, and then the ellipticity increased to the value of the N state in the second observable phase. These processes were also seen in the kinetic refolding measurement of the protein using CD at 222 nm (*8*). In the measurement at 232.5 nm, however, there was no overshoot in the first phase, and a biphasic process with decreasing ellipticity was observed. The rate constants of the two phases were calculated by global fitting of the 10 kinetic curves at different wavelengths (see below), and they were as follows: $k_1 = 22 \pm 2$ s$^{-1}$ and $k_2 = 0.53 \pm 0.02$ s$^{-1}$.

We also assessed the unfolding reaction of the protein using the stopped-flow CD apparatus, and Figure 3c shows a typical unfolding curve, in which the unfolding reaction was initiated by a jump in GdnHCl concentration from 0 to 7.66 M. As a result, 80% of the total ellipticity change expected from the equilibrium unfolding curve was kinetically observed. The change was represented as a single-exponential process, and its rate constant $k$ equaled 1.06 ± 0.09 s$^{-1}$. Twenty percent of the total ellipticity change occurred within the dead time of the stopped-flow apparatus (15 ms). This may have been due to the presence of a burst phase in the unfolding kinetics, or the CD change caused by a change in the solvent condition.

*CD Spectra of $I_{burst}$ and $I_{second}$, and Their Relationship with the Equilibrium I State.* To obtain CD spectra of the two kinetic intermediates, $I_{burst}$ and $I_{second}$, that accumulated during the refolding reaction, we assessed the refolding reactions of canine lysozyme using CD at 10 different wavelengths from 215 to 240 nm. All of the observed curves were biphasic and analyzed by nonlinear least-squares calculations. We performed a global fitting in which the 10 kinetic curves at different wavelengths were fitted simultaneously, and obtained the two rate constants shown above. The amplitudes of the two exponential terms are given in Table 1. At all wavelengths, the theoretical curves calculated from the global fitting represented well the experimental data measured by CD (see panels a and b of Figure 3). The ellipticity values of $I_{burst}$ [i.e., $A_\infty + A_1 + A_2$ (□)] and those of $I_{second}$ extrapolated to time zero [i.e., $A_\infty + A_2$ (●)] are shown in Figure 2a.

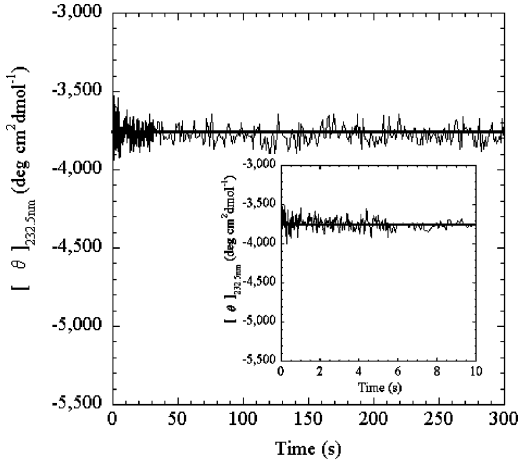


FIGURE 4: CD ellipticity at 232.5 nm as a function of time when the refolding of canine lysozyme was carried out by a GdnHCl concentration jump from 7.0 to 3.85 M. The absence of the observed kinetics indicates that the CD change from the unfolded state to the intermediate state occurs suddenly within the dead time of the measurement. The inset of the figure shows the curve in the expanded scale.

We also calculated the spectrum of the pure I state at 3.85 M GdnHCl from the experimentally observed spectra at GdnHCl concentrations of 0, 3.85, and 7.14 M. We first assume that the ellipticity at wavelength $\lambda$ observed in the equilibrium unfolding measurements [$A_{obs}(\lambda)$] is the sum of contributions from the pure N, I, and U states [$A_N(\lambda)$, $A_I(\lambda)$, and $A_U(\lambda)$, respectively]

$$A_{obs}(\lambda) = f_N A_N(\lambda) + f_I A_I(\lambda) + f_U A_U(\lambda) \quad (3)$$

where $f_N$, $f_I$, and $f_U$ are the fractions of the N, I, and U states, respectively, at 3.85 M GdnHCl, and these values were theoretically calculated from the equilibrium unfolding parameters obtained previously (Figure 1a; *8*). Thus, $A_I(\lambda)$ can be calculated by the following formula:

$$A_I(\lambda) = \frac{A_{obs}(\lambda) - A_N(\lambda) f_N - A_U(\lambda) f_U}{f_I} \quad (4)$$

Here, we take the observed ellipticity values at wavelength $\lambda$ at 0 and 7.14 M GdnHCl to be $A_N(\lambda)$ and $A_U(\lambda)$, respectively. The spectrum thus obtained is shown in Figure 2a (dotted line). The spectrum is more similar to the spectrum of $I_{burst}$ than to the spectrum of $I_{second}$, suggesting the equivalence of $I_{burst}$ and I.

To further investigate which intermediate, $I_{burst}$ or $I_{second}$, is equivalent to the I state, the refolding reaction from the U state to the I state was investigated by the stopped-flow CD (Figure 4). The reaction was induced by a GdnHCl concentration jump from 7.0 to 3.85 M. Eighty-four percent of the protein molecules are in the I state at 3.85 M GdnHCl (Figure 1). The ellipticity change at 232.5 nm was complete within the dead time of the stopped-flow instrument, and no change was observed in the time range up to 331 s after the reaction started. This result thus further supports the possibility that

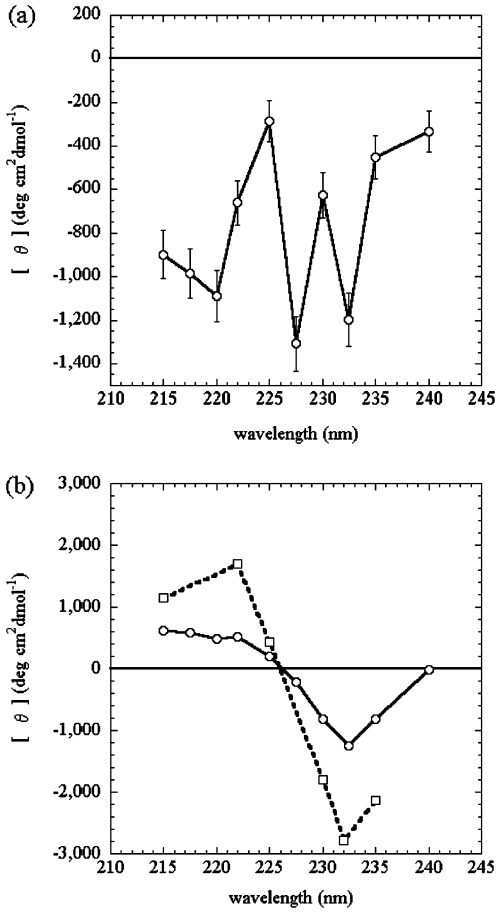


FIGURE 5: (a) Kinetic difference CD spectrum of the refolding of canine lysozyme from $I_{burst}$ to $I_{second}$ (−○−). (b) Kinetic difference CD spectrum of the refolding of canine lysozyme from $I_{second}$ to N at 0.61 M GdnHCl at pH 7.0 and 25 °C (−○−). The error bars are the standard errors obtained by the nonlinier least-squares method. The kinetic difference CD spectrum of the refolding of equine lysozyme from the burst-phase intermediate to the native state is also shown (---□---). The data were calculated from the spectra reported previously (*9*).

the I state is formed rapidly within the dead time, and hence, the I state is equivalent to $I_{burst}$.

*Kinetic Difference CD Spectra.* The two-exponential fit of the refolding curves measured at 10 different wavelengths provides kinetic difference CD spectra for the phase from $I_{burst}$ to $I_{second}$, and for the phase from $I_{second}$ to N. The difference spectra are related to fractional changes in secondary and/or tertiary structure components, which may occur during the kinetic phases. The difference spectra for the phase from $I_{burst}$ to $I_{second}$ and for the phase from $I_{second}$ to N are given by the wavelength dependence of the amplitudes, $-A_1$ and $-A_2$, respectively. The difference spectra thus obtained are shown in Figure 5. The phase from $I_{burst}$ to $I_{second}$ shows an increase in the negative ellipticities. In the difference spectrum from $I_{second}$ to N, positive and negative bands centered around 226 nm were observed.

## DISCUSSION

*Relationship between the Kinetic Intermediates and the Equilibrium Intermediate.* The unfolding intermediate (I) of recombinant canine milk lysozyme observed in the equilibrium unfolding induced by heat or GdnHCl is remarkably more stable and more structured than the unfolding intermediates observed in other proteins in the lysozyme and α-lactalbumin family (*6*−*8*). Furthermore, there are at least two kinetic intermediates during the refolding of canine lysozyme: the burst-phase (first) intermediate ($I_{burst}$) and the second kinetic intermediate ($I_{second}$) that accumulates after the burst phase (*8*). However, the structural characteristics of $I_{burst}$ and $I_{second}$ remain poorly understood. In this study, we assessed the kinetic refolding reactions using CD spectroscopy at 10 different wavelengths, and obtained the CD spectra of $I_{burst}$ and $I_{second}$. Comparison of these CD spectra with the spectrum calculated for the pure I state, as well as the sudden CD change in the refolding from the unfolded (U) state to the I state, indicates that $I_{burst}$ is equivalent to the I state.

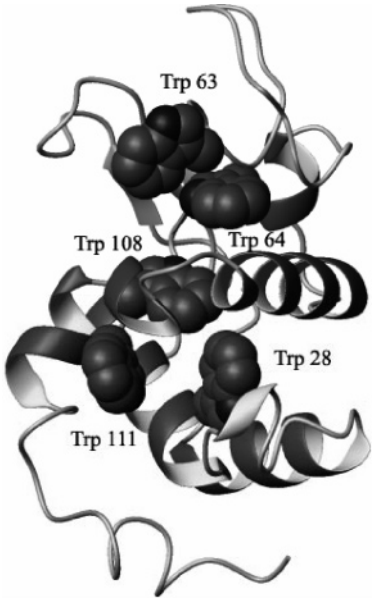


FIGURE 6: Schematic representation of the three-dimensional structure of canine lysozyme based on the coordinates of the A-chain in PDB entry 1EL1. Five tryptophan side chains are shown as space filling diagrams. This figure was prepared with MOLMOL (*27*).

*Possible Origins of the Kinetic Difference CD Spectra.* The kinetic CD spectra represent changes in the structure of canine milk lysozyme in every kinetic phase. In the phase from $I_{burst}$ to $I_{second}$, the ellipticity of each wavelength decreased, suggesting an increase in secondary structure content. In the difference spectrum between N and $I_{second}$, positive and negative bands with an isoellipticity point around 226 nm were observed. This kind of difference spectrum was previously observed in the first phase of refolding of dihydrofolate reductase (DHFR), and it is known to be caused by exciton coupling of a pair of tryptophan residues, Trp47 and Trp74, involved in the exciton pair in DHFR (*13*, *14*). The difference spectrum of DHFR also had positive and negative bands with an isoellipticity point around 226 nm, with intensities similar to those observed here. It is thus likely that the difference spectrum between N and $I_{second}$ for canine lysozyme is also caused by the exciton coupling of a pair of adjusted tryptophan residues. In fact, when we look at the structure of canine lysozyme obtained from X-ray crystallography, there exist two such pairs of tryptophan residues whose side chains are close to each other (Trp63 and Trp64, and Trp28 and Trp108) (see Figure 6). Therefore, the phase from $I_{second}$ to N may represent the specific packing of one

or both of these pairs of tryptophan residues, which leads to the exciton coupling CD bands. However, because the intensities of the two bands are not equal to each other, there may be some other contributions to the difference spectrum.

In the refolding reaction of equine lysozyme, the burst-phase intermediate was also equivalent to the equilibrium unfolding intermediate, but no other kinetic intermediate was observed after the burst phase (*9*). When we compare the amino acid sequences of equine and canine lysozyme, however, the positions of tryptophan residues are perfectly preserved. We thus calculated the difference spectrum between the native state and the burst-phase intermediate from the spectra of these states of equine lysozyme reported previously (*9*). The difference spectrum thus obtained resembles that of the canine protein between N and $I_{second}$ [Figure 5b (□)]. This result is thus consistent with the notion that this type of difference spectrum may arise from an exciton pair of adjusted tryptophan residues, and the burst-phase intermediate of the equine protein may correspond to $I_{second}$ of the canine protein.

Morozova-Roche et al. (*15*) also studied the refolding kinetics of equine lysozyme using hydrogen exchange pulse labeling experiments coupled with nuclear magnetic resonance (NMR) spectroscopy and stopped-flow optical methods. In their results, the rate constant of the kinetic phase observed at 225 nm in the far-UV CD is similar to that of the C-helix protection kinetics. Moreover, the slow phase of the biphasic kinetics of refolding, as monitored by the protection of the Trp108 peptide amide and indole NH protons, was characterized by rate constants in the same range observed here. It has been shown that Trp108 and other aromatic residues from the A-, B-, and D-helix cluster make contacts with the C-helix (*16*). They have thus concluded that the structural rearrangements in the core area occur at the final phase of refolding, bringing aromatic residues and Trp108 in particular from non-native into nativelike conformations. When we take into account these results as well as the results presented here, the Trp28−Trp108 pair might be a candidate contributing to the exciton coupling band in the far-UV CD spectra.

*A Scheme of the Refolding of Canine Milk Lysozyme.* A schematic representation of the refolding of canine milk lysozyme can be given by

$$U \xrightarrow{\text{phase 1}} I_{burst} \xrightarrow{\text{phase 2}} I_{second} \xrightarrow{\text{phase 3}} N$$

In the refolding, the burst-phase intermediate ($I_{burst}$) whose structure resembles that of the equilibrium intermediate accumulates within the dead time of the stopped-flow apparatus (phase 1). In this step, most of the nativelike secondary structures and some of the hydrophobic cores are constructed (*8*). After the burst phase, the secondary structures are rearranged, and then the second kinetic intermediate ($I_{second}$) is observed (phase 2). Finally, the aromatic side chains are packed specifically, which leads to the appearance of the exciton coupling bands of adjacent tryptophan residues, and the molecules become the native state (N) (phase 3).

*Comparison with Other Studies.* Van Dael et al. (*17*) assessed the kinetic refolding reaction of canine milk lysozyme with a GdnHCl concentration jump from 6.0 to 0.54 M using CD spectroscopy at 225 nm. In contrast to our observations, they observed only single-exponential kinetics with a rate constant $k$ of 4.7 $s^{-1}$ after the burst phase. There are some differences between their experimental conditions and ours. First, they measured the kinetics in 10 mM Tris, 80 mM NaCl, and 10 mM $CaCl_2$ at pH 7.5. On the other hand, we measured the kinetics in 50 mM sodium cacodylate buffer (pH 7.0) that contained 50 mM NaCl and 1 mM $CaCl_2$. The differences in the concentrations of NaCl and calcium ion may have caused changes in the CD spectral properties and/or the stabilities of the intermediates. As a consequence, the difference in ellipticity between $I_{burst}$ and $I_{second}$ at 225 nm might have been smaller than that in our measurements such that Van Dael and colleagues could not detect $I_{second}$. Second, they used authentic canine milk lysozyme purified from fresh canine milk instead of recombinant canine milk lysozyme expressed in *E. coli* cells, which possesses an extra methionine residue at the amino terminus. The presence or absence of the methionine residue might affect the refolding kinetics of the protein, although it has been shown that this does not influence the refolding kinetics in α-lactalbumin (*18*, *19*).

There are certain proteins in which a second kinetic intermediate is observed after a burst-phase intermediate in the refolding process. In the kinetic refolding of apomyoglobin, two intermediates, Ia and Ib, accumulate, and the anion-induced, more-structured molten globule state observed at equilibrium may be related to the late intermediate, Ib (*20*). In hen lysozyme, no equilibrium molten globule state is detected under most conditions. However, in the refolding process, there exist a number of kinetic intermediates. This protein folds on both fast and slow tracks at pH 5.2 and 20 °C, and two distinct folding intermediates are observed on the slow folding track. These are the burst-phase intermediate and a late-folding intermediate (α-domain intermediate) that accumulates maximally at 100 ms of refolding and shows significant hydrogen exchange protection in the α-domain (*21*, *22*). The burst-phase intermediate may be consistent with the burst-phase molten globule state observed in α-lactalbumin (*23*). The late-folding intermediate, having the characteristics of the molten globule state, is more structured than the burst-phase intermediate (*21*). The refolding process of canine lysozyme and those for the other proteins described above are consistent with a hierarchical model of protein folding; i.e., the existence of two distinctive energetic barriers along the pathway for formation of the native state from the burst-phase intermediate may account for the accumulation of a more structured late kinetic intermediate that is productive and placed along the folding pathway (*24*−*26*).

## ACKNOWLEDGMENT

We thank Mr. Takayuki Morimoto for his help in the preparation of canine milk lysozyme.

## REFERENCES

1. Kim, P. S., and Baldwin, R. L. (1990) Intermediates in the folding reactions of small proteins, *Annu. Rev. Biochem. 59*, 631−660.
2. Arai, M., and Kuwajima, K. (1996) Rapid formation of a molten globule intermediate in refolding of α-lactalbumin, *Folding Des. 1*, 275−287.
3. Ptitsyn, O. B. (1987) Protein folding: Hypothesis and experiments, *J. Protein Chem. 6*, 273−293.
4. Kuwajima, K. (1989) The molten globule state as a clue of understanding the folding and cooperativity of globular-protein structure, *Proteins 6*, 87−103.

5. Ptitsyn, O. B., Pain, R. H., Semisotnov, G. V., Zerovnik, E., and Razgulyaev, O. I. (1990) Evidence for a molten globule state as a general intermediate in protein folding, *FEBS Lett. 262*, 20−24.
6. Koshiba, T., Yao, M., Kobashigawa, Y., Demura, M., Nakagawa, A., Tanaka, I., Kuwajima, K., and Nitta, K. (2000) Structure and thermodynamics of the extraordinarily stable molten globule state of canine milk lysozyme, *Biochemistry 39*, 3248−3257.
7. Kobashigawa, Y., Demura, M., Koshiba, T., Kumaki, Y., Kuwajima, K., and Nitta, K. (2000) Hydrogen exchange study of canine milk lysozyme: Stabilization mechanism of the molten globule, *Proteins 40*, 579−589.
8. Nakao, M., Arai, M., Koshiba, T., Nitta, K., and Kuwajima, K. (2003) Folding mechanism of canine milk lysozyme studied by circular dichroism and fluorescence spectroscopy, *Spectroscopy 17*, 183−193.
9. Mizuguchi, M., Arai, M., Ke, Y., Nitta, K., and Kuwajima K. (1998) Equilibrium and kinetics of the folding of equine lysozyme studied by circular dichroism spectroscopy, *J. Mol. Biol. 283*, 265−277.
10. Pace, C. N. (1986) Determination and analysis of urea and guanidine hydrochloride denaturation curves, *Methods Enzymol. 131*, 266−280.
11. Kikuchi, M., Kawano, K., and Nitta, K. (1998) Calcium-binding and structural stability of echidna and canine milk lysozyme, *Protein Sci. 7*, 2150−2155.
12. Ikeguchi, M., Kuwajima, K., and Sugai, S. (1986) $Ca^{2+}$-induced alteration in the unfolding behavior of α-lactalbumin, *J. Biochem. 99*, 1191−1201.
13. Kuwajima, K., Garvey, E. P., Finn, B. E., Matthews, C. R., and Sugai, S. (1991) Transient intermediates in the folding of dihydrofolate reductase as detected by far-ultraviolet circular dichroism spectroscopy, *Biochemistry 30*, 7693−7703.
14. Woody, R. W., and Dunker, A. K. (1996) Aromatic and cystine side-chain CD in proteins, *Circular Dichroism and the Conformational Analysis of Biomolecules*, pp 109−157, Plenum Press, New York.
15. Morozova-Roche, L. A., Jones, J. A., Noppe, W., and Dobson, C. M. (1999) Independent nucleation and heterogeneous assembly of structure during folding of equine lysozyme, *J. Mol. Biol. 289*, 1055−1073.
16. Morozova-Roche, L. A., Arico-Muendel, C. C., Haynie, D. T., Emelyanenko, V. I., Van Dael, H., and Dobson, C. M. (1997) Structural characterisation and comparison of the native and A-states of equine lysozyme, *J. Mol. Biol. 268*, 903−921.
17. Van Dael, H., Haezebrouck, P., and Joniau, M. (2003) Equilibrium and kinetic studies on folding of canine milk lysozyme, *Protein Sci. 12*, 609−619.
18. Chaudhuri, T. K., Horii, K., Yoda, T., Arai, M., Nagata, S., Terada, T. P., Uchiyama, H., Ikura, T., Tsumoto, K., Kataoka, H., Matsushima, M., Kuwajima, K., and Kumagai, I. (1999) Effect of the extra N-terminal methionine residue on the stability and folding of recombinant α-lactalbumin expressed in *Escherichia coli*, *J. Mol. Biol. 285*, 1179−1194.
19. Chaudhuri, T. K., Arai, M., Terada, T. P., Ikura, T., and Kuwajima, K. (2000) Equilibrium and kinetic studies on folding of the authentic and recombinant forms of human α-lactalbumin by circular dichroism spectroscopy, *Biochemistry 39*, 15643−15651.
20. Jamin, M., and Baldwin, R. L. (1998) Two forms of the pH 4 folding intermediate of apomyoglobin, *J. Mol. Biol. 276*, 491−504.
21. Matagne, A., and Dobson, C. M. (1998) The folding process of hen lysozyme: A perspective from the 'new view', *Cell. Mol. Life Sci. 54*, 363−371.
22. Segel, D. J., Bachmann, A., Hofrichter, J., Hodgson, K. O., Doniach, S., and Kiefhaber, T. (1999) Characterization of transient intermediates in lysozyme folding with time-resolved small-angle X-ray scatterin, *J. Mol. Biol. 288*, 489−499.
23. Gladwin, S. T., and Evans, P. A. (1996) Structure of very early protein folding intermediates: New insights through a variant of hydrogen exchange labeling, *Folding Des. 1*, 407−417.
24. Arai, M., and Kuwajima, K. (2000) The role of the molten globule state in protein folding, *Adv. Protein Chem. 53*, 209−282.
25. Kuwajima, K., and Arai, M. (2000) The molten globule state: The physical picture and biological significance, in *Mechanisms of Protein Folding* (Pain, R. H., Ed.) 2nd ed., pp 138−174, Oxford University Press, New York.
26. Kamagata, K., Arai, M., and Kuwajima, K. (2004) Unification of the folding mechanisms of non-two-state and two-state proteins, *J. Mol. Biol. 339*, 951−965.
27. Koradi, R., Billeter, M., and Wüthrich, K. (1996) MOLMOL: A program for display and analysis of macromolecular structures, *J. Mol. Graphics 14*, 51−55.

BI050082+